

O. V. PYLYPENKO, A. V. DORONIN, N. B. GOREV, I. F. KODZHESPIROVA

**TWO-PROBE MEASUREMENTS OF THE DISPLACEMENT OF MECHANICAL OBJECTS OVER A WIDE RANGE OF THE REFLECTION COEFFICIENT**

*Institute of Technical Mechanics  
of the National Academy of Sciences of Ukraine and the State Space Agency of Ukraine,  
15 Leshko-Popel St., Dnipro 49005, Ukraine; e-mail: ifk56@ukr.net*

This paper addresses a two-probe implementation of microwave interferometry for measurement of the displacement of a target with an unknown reflection coefficient. The aim of this paper is to improve the measurement accuracy over a wide range of the target reflection coefficient. The measurement error as a function of the interprobe distance, the free-space operating wavelength, the width of the broad wall of the waveguide section with the probes, and the target reflection coefficient is analyzed with the inclusion of variations of the currents of the semiconductor detectors connected to the probes from their theoretical values. As the free-space operating wavelength increases, the measurement error passes through a minimum for reflection coefficients close to unity and increases monotonically for smaller reflection coefficients. This behavior of the error is due to the fact that

© O. V. Pylypenko, A. V. Doronin, N. B. Gorev, I. F. Kodzhespirova, 2020

. – 2020. – 2.

with increasing free-space operating wavelength and/or reflection coefficient the inherent error of two-probe measurements decreases, while the error caused by variations of the detector currents from their theoretical values increases. A measurement error reduction technique is proposed. The technique consists in changing the free-space operating wavelength in accordance with the measured reflection coefficient. In comparison with the conventional operating mode, in which the interprobe distance is equal to the one eighth of the guided wavelength, the proposed technique offers a significant reduction in the measurement error for reflection coefficients close to unity. As distinct from an existing technique that uses a fixed value of the interprobe distance to guided wavelength ratio smaller than  $1/8$ , the proposed technique is free from such a drawback as a marked increase in the measurement error at rather small reflection coefficients. The results reported in this paper may be used in the development of microwave displacement sensors for various classes of vibration protection and workflow control systems.

**Keywords:** complex reflection coefficient, displacement, electrical probe, microwave interferometry, semiconductor detector, waveguide section.

Microwave interferometry is an ideal means for displacement measurement in various engineering applications [1]. This is due to its ability to provide fast non-contact measurements, applicability to dusty or smoky environments (as distinct from laser Doppler sensors [2 – 4] or vision-based systems using digital image processing techniques [5]), and simple hardware implementation. In microwave interferometry, the displacement of the object under measurement (target) is extracted from the phase shift between the signal reflected from the target and the reference signal. At present, this phase shift is usually determined using special hardware incorporating a power divider and a phase-detecting processor, which is an analog [6] or a digital [7] quadrature mixer. In doing so, measures have to be taken to minimize the nonlinear phase response of the quadrature mixer, which is caused by its phase and amplitude unbalances.

A two-probe displacement measurement technique was proposed in [8]. In that technique, the quadrature signals needed for the determination of the phase shift are extracted from the outputs of two probes placed in a waveguide section one eighth of the guided operating wavelength  $\lambda_g$  apart. In hardware implementation, that technique is far simpler than conventional techniques based on quadrature mixing [6, 7]. Its distinctive feature is the possibility of displacement measurement at an unknown reflection coefficient with as few as two probes, while since the classic text by Tischer [9] three probes have still been used to determine or eliminate the unknown reflection coefficient [10, 11]. Theoretically, the technique gives the exact value of the displacement for reflection coefficients (at the location of the probes) no greater than  $1/\sqrt{2}$  and in the general case determines it to a worst-case accuracy of about 4.4% of the free-space operating wavelength. In [12] it was shown that the measurement error can be reduced by going from the conventional  $\lambda_g/8$  to a shorter interprobe distance. However, decreasing the interprobe distance increases the error that is due to variations of the detector currents from their theoretical values, and this error increases with decreasing reflection coefficient. The aim of this paper is to improve the measurement accuracy over a wide range of the target reflection coefficient. This aim is achieved by changing the operating wavelength in accordance with the measured reflection coefficient.

Consider two probes, 1 and 2, with square-law semiconductor detectors placed  $l$  apart in a waveguide section between a microwave oscillator and a target so that probe 2 is closer to the target (Fig. 1).

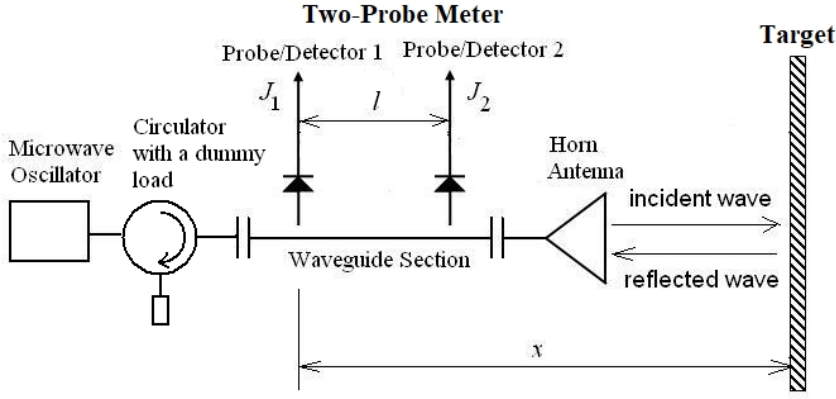


Fig. 1

The detector currents  $J_1$  and  $J_2$  (normalized to their matched-load values) are [12]

$$J_1 = 1 + R^2 + 2R \cos \psi, \quad (1)$$

$$J_2 = 1 + R^2 + 2R \sin(\psi - \beta), \quad (2)$$

$$\psi = \frac{4\pi x}{\lambda} + \phi, \quad \beta = \frac{\pi}{2} \left( \frac{l - \lambda_g/8}{\lambda_g/8} \right),$$

where  $R$  and  $\psi$  are the magnitude and phase of the unknown complex reflection coefficient at the location of probe 1 (for simplicity, in the following discussion the magnitude of the complex reflection coefficient will be referred to as the reflection coefficient),  $x$  is the distance between the target and probe 1,  $\lambda$  is the free-space operating wavelength, and the term  $\phi$ , which is governed by the waveguide section and horn antenna geometry and the phase shift caused by the reflection, does not depend on the distance  $x$ .

The guided operating wavelength  $\lambda_g$  is related to the free-space operating wavelength  $\lambda$  as follows:

$$\lambda_g = \frac{\lambda}{\sqrt{1 - \left(\frac{\lambda}{2W}\right)^2}},$$

where  $W$  is the width of the waveguide's broad wall.

Let  $\lambda_0$  be the free-space operating wavelength such that  $l = \lambda_g(\lambda_0)/8$ . Then the expression for  $\beta$  as a function of  $\lambda$  will be

$$\beta(\lambda) = \frac{\pi}{2} \left[ \frac{\lambda_0}{\lambda} \sqrt{\frac{1 - (\lambda/2W)^2}{1 - (\lambda_0/2W)^2}} - 1 \right].$$

Let it be desired to find the displacement  $\Delta x(t)$  of the target relative to its initial position  $x(t_0)$  from the measured currents  $J_1(t)$  and  $J_2(t)$ . As will be shown

below, this displacement can be unambiguously determined from the quadrature signals  $\cos \psi$  and  $\sin \psi$ . From Eqs. (1) and (2) we have

$$\cos \psi = \frac{a_1 - R^2}{2R}, \quad (3)$$

$$\sin \psi = \frac{a_2 + a_1 \sin \beta - R^2(1 + \sin \beta)}{2R \cos \beta}, \quad (4)$$

where  $a_1 = J_1 - 1$ ,  $a_2 = J_2 - 1$ .

Combining the squares of Eqs, (3) and (4) gives the biquadratic equation in  $R$

$$R^4 - [a_1 + a_2 + 2(1 - \sin \beta)]R^2 + \frac{a_1^2 + a_2^2 + 2a_1a_2 \sin \beta}{2(1 + \sin \beta)} = 0. \quad (5)$$

This equation has two positive roots. Let  $R_1$  and  $R_2$  be the greater and the smaller positive root, respectively. Clearly one of the two roots is extraneous.

Using Eqs. (3) and (4), the absolute term of Eq. (5) may be brought to the form

$$\frac{a_1^2 + a_2^2 + 2a_1a_2 \sin \beta}{2(1 + \sin \beta)} = R^2 \left\{ R^2 + 2R[\cos \psi + \sin(\psi - \beta)] + 2(1 - \sin \beta) \right\}.$$

Since the absolute term of a biquadratic equation is the product of its roots, for the extraneous root  $R_{ext}$  we have

$$R_{ext} = \left\{ R^2 + 2R[\cos \psi + \sin(\psi - \beta)] + 2(1 - \sin \beta) \right\}^{1/2}. \quad (6)$$

On rearrangement, the expression for  $R_{ext}$  becomes

$$R_{ext} = \left[ R^2 + 4R_0R \sin(\psi + \gamma_1) + 4R_0^2 \right]^{1/2}, \quad (7)$$

where  $R_0 = \sqrt{(1 - \sin \beta)/2}$  and  $\gamma_1 = \arcsin R_0$ .

Using Eq. (7), it can be shown that  $R_{ext}$  and  $R$  are compared as follows:  $R_{ext} \geq R$  for  $\sin(\psi + \gamma_1) \geq -R_0/R$  and  $R_{ext} < R$  for  $\sin(\psi + \gamma_1) < -R_0/R$ . Since by definition  $R_1 \geq R_2$ , for the reflection coefficient  $R$  we have

$$R = \begin{cases} R_2, & \sin(\psi + \gamma_1) \geq -R_0/R, \\ R_1, & \sin(\psi + \gamma_1) < -R_0/R. \end{cases}$$

First consider the case  $R \leq R_0$ . In this case the condition  $\sin(\psi + \gamma_1) \geq -R_0/R$  is met at any  $\psi$ , and thus the reflection coefficient  $R$  is unambiguously determined from Eq. (5) as its root  $R_2$ , thus allowing  $\cos \psi$  and  $\sin \psi$  to be unambiguously determined from Eqs. (3) and (4). Given  $\cos \psi$  and  $\sin \psi$ , the target displacement can be extracted using the phase unwrapping method, which is a powerful tool to resolve the phase ambiguity problem in a number of applications [13, 14]. The

displacement  $\Delta x$  of the target at time  $t_n$ ,  $n=0,1,2,\dots$ , from its initial position  $x(t_0)$  can be found by the following phase unwrapping algorithm [15]

$$\varphi(t_n) = \begin{cases} \arctan \frac{\sin\psi(t_n)}{\cos\psi(t_n)}, & \sin\psi(t_n) \geq 0, \cos\psi(t_n) \geq 0, \\ \arctan \frac{\sin\psi(t_n)}{\cos\psi(t_n)} + \pi, & \cos\psi(t_n) < 0, \\ \arctan \frac{\sin(t_n)}{\cos\psi(t_n)} + 2\pi, & \sin\psi(t_n) < 0, \cos\psi(t_n) \geq 0, \end{cases} \quad (8)$$

$$\Delta\varphi(t_n) = \varphi(t_n) - \varphi(t_{n-1}), \quad (9)$$

$$\theta(t_n) = \begin{cases} 0, & n = 0, \\ \theta(t_{n-1}) + \Delta\varphi(t_n), & |\Delta\varphi(t_n)| \leq \pi, \quad n = 1, 2, \dots, \\ \theta(t_{n-1}) + \Delta\varphi(t_n) - 2\pi \operatorname{sgn}[\Delta\varphi(t_n)], & |\Delta\varphi(t_n)| > \pi, \quad n = 1, 2, \dots, \end{cases} \quad (10)$$

$$\Delta x(t_n) = \frac{\lambda}{4\pi} \theta(t_n), \quad n = 0, 1, 2, \dots, \quad (11)$$

where  $\varphi$  and  $\theta$  are the wrapped and the unwrapped phase, respectively.

In the case  $R > R_0$ , the root  $R_2$  will not always be equal to  $R$ , but, as will be shown below, the displacement can also be determined to sufficient accuracy assuming that  $R = R_2$ . As shown above, the root  $R_2$  is extraneous if  $\sin(\psi + \gamma_1) < -R_0/R$ . In terms of the wrapped phase  $\varphi$ , this condition becomes

$$\varphi_1 < \varphi < \varphi_2,$$

Where  $\varphi_1 = \pi + \gamma_2 - \gamma_1$ ,  $\varphi_2 = 2\pi - \gamma_1 - \gamma_2$ ,  $\gamma_2 = \arcsin \frac{R_0}{R}$ .

In the case  $l \leq \lambda_g/8$  ( $1/\sqrt{2} \leq R_0 < 1$ ), we have

$$\frac{\pi}{4} \leq \gamma_1 \leq \gamma_2 < \frac{\pi}{2},$$

whence it follows that the angles  $\varphi_1$  and  $\varphi_2$  are in the third quadrant.

From Eq. (7) it follows that the minimum value of the extraneous root is

$$R_{ext \min} = \left[ R^2 - 4R_0R + 4R_0^2 \right]^{1/2} = 2R_0 - R. \quad (12)$$

Because of this, if the root  $R_2$  is less than  $R_{ext \min}$ , it will certainly be equal to the actual reflection coefficient  $R$ . Otherwise, any value between  $R_{ext \min}$  and 1 may be the actual reflection coefficient.

If the extraneous root  $R_{ext}$  is taken as the reflection coefficient, Eqs. (3) and (4) for  $\cos \psi$  and  $\sin \psi$  will give their apparent values, for which in view of Eqs. (6) and (7) we will have

$$\cos \psi_{ap} = -\frac{1 + R \sin(\varphi - \beta) - \sin \beta}{R_{ext}},$$

$$\sin \psi_{ap} = -\frac{1 + R \cos \varphi - \sin \beta [\sin \beta - R \sin(\varphi - \beta)]}{R_{ext} \cos \beta}.$$

Eq. (8) for the determination of the wrapped phase includes the inverse tangent of the ratio  $\sin \psi / \cos \psi$ . So consider the function  $F(\varphi) = \sin \psi_{ap} / \cos \psi_{ap}$ ,  $\varphi_1 < \varphi < \varphi_2$

$$F(\varphi) = \frac{1 + R \cos \varphi - \sin \beta [\sin \beta - R \sin(\varphi - \beta)]}{\cos \beta [1 + R \sin(\varphi - \beta) - \sin \beta]}.$$

For its derivative with respect to  $\varphi$  we have

$$F'(\varphi) = \frac{R^2 \left[ -2 \frac{R_0}{R} \sin(\varphi + \gamma_1) - 1 \right]}{[1 + R \sin(\varphi - \beta) - \sin \beta]^2} > \frac{R^2 [2R_0^2 - 1]}{[1 + R \sin(\varphi - \beta) - \sin \beta]^2} \geq 0.$$

Thus the apparent wrapped phase  $\varphi_{ap}$  is a steadily increasing function of the actual wrapped phase  $\varphi$ . Since at the points  $\varphi = \varphi_1$  and  $\varphi = \varphi_2$  the apparent and the actual phase coincide, this means that the apparent phase also lies between  $\varphi_1$  and  $\varphi_2$ , i. e., in the third quadrant. Thus the phase error  $\Delta \varphi_{er} = \varphi_{ap} - \varphi$  is

$$\Delta \varphi_{er}(\varphi) = \begin{cases} 0, & 0 \leq \varphi \leq \varphi_1, \varphi_2 \leq \varphi \leq 2\pi \\ \arctan F(\varphi) + \pi - \varphi, & \varphi_1 < \varphi < \varphi_2. \end{cases}$$

The phase error  $\Delta \varphi_{er}(\varphi)$  has a negative minimum at  $\varphi_3 = \pi + \gamma_3 - \gamma_1$  and a positive maximum at  $\varphi_4 = 2\pi - \gamma_3 - \gamma_1$  where

$$\gamma_3 = \arcsin \frac{R^2 + 2R_0^2}{3RR_0}.$$

The minimum value of the phase error  $\Delta \varphi_{er}(\varphi)$  at  $\varphi = \varphi_3$  is

$$\Delta \varphi_{er \min} = \arctan \frac{\cos \beta - R \cos(\gamma_3 - \gamma_1 - \beta)}{1 - R \sin(\gamma_3 - \gamma_1 - \beta)} + \gamma_1 - \gamma_3,$$

and its maximum value at  $\varphi = \varphi_4$  is

$$\Delta \varphi_{er \max}(r) = \arctan \frac{\cos \beta + R \cos(\beta + \gamma_1 + \gamma_3)}{1 - R \sin(\beta + \gamma_1 + \gamma_3)} + \gamma_1 + \gamma_3 - \pi.$$

As can be seen from Eqs. (9) – (11), the displacement error is governed only by the phase error at the initial and the current measurement point because the intermediate points cancel one another. Because of this, the maximum displacement error will be

$$|\Delta x_{er}|_{\max} = \frac{\lambda}{4\pi} (\Delta\varphi_{er \max} - \Delta\varphi_{er \min}).$$

Fig. 2 shows the ratio  $|\Delta x_{er}|_{\max} / \lambda_0 = \frac{\lambda}{4\pi\lambda_0} (\Delta\varphi_{er \max} - \Delta\varphi_{er \min}) \equiv \delta_{\max}$  versus  $R$  at different values of the ratio  $\lambda / \lambda_0$  for a standard 23 mm x 10 mm waveguide ( $W = 23$  mm) and  $\lambda_0 = 3$  cm.

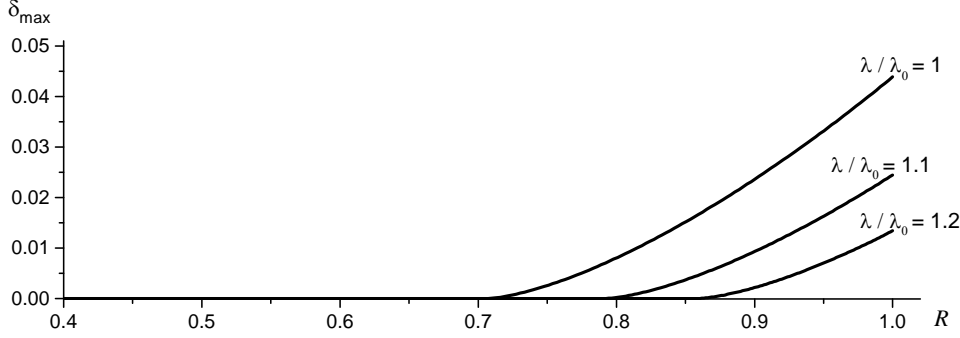


Fig. 2

As illustrated, the error  $\delta_{\max}$  decreases rapidly with increasing  $\lambda$ . However, increasing  $\lambda$  decreases the ratio  $l / \lambda_g$ . This, in its turn, increases the contribution of the error caused by variations of the detector currents from their theoretical values given by Eqs. (1) and (2) (such variations may be due to the effect of the reflecting surface shape and orientation and the antenna radiation pattern on the reflected wave, electromagnetic noise, etc.). To demonstrate, let us bring the absolute term of Eq. (5) to the form:

$$\frac{a_1^2 + a_2^2 + 2a_1a_2 \sin \beta}{2(1 + \sin \beta)} = \frac{(J_{1th} - J_{2th} + \Delta J_1 - \Delta J_2)^2}{2(1 + \sin \beta)} + (J_{1th} + \Delta J_1 - 1)(J_{2th} + \Delta J_2 - 1),$$

where  $\Delta J_1$  and  $\Delta J_2$  are variations of the detector currents from their theoretical values  $J_{1th}$  and  $J_{2th}$ .

As the ratio  $l / \lambda_g$  tends to zero,  $J_{1th} - J_{2th}$  and  $1 + \sin \beta$  tend to zero too, and thus the contribution of the current variations  $\Delta J_1$  and  $\Delta J_2$  becomes dominating.

Calculations were conducted to find out an advisable value of the ratio  $\lambda / \lambda_0$ . In the calculations, the determination of the relative displacement of a target executing a harmonic vibratory motion was simulated. In doing so, variations of the detector currents from their theoretical values were modeled by random current noise. The distance  $x$  of the target to probe 1 and the detector currents  $J_1$  and  $J_2$  were simulated as

$$x(t) = x_0 + A \sin(2\pi t/T),$$

$$\psi = \psi_0 + \frac{4\pi}{\lambda} A \sin(2\pi t/T), \quad \psi_0 = \phi + \frac{4\pi x_0}{\lambda},$$

$$J_1 = (1 + R^2 + 2R \cos \psi)(1 + A_n r),$$

$$J_2 = [1 + R^2 + 2R \sin(\psi - \beta)](1 + A_n r),$$

where  $t$  is the time,  $A$  and  $T$  are the target vibration amplitude and period,  $x_0$  and  $\psi_0$  are the distance  $x$  and the phase  $\psi$  at  $t = 0$ ,  $A_n$  is the noise amplitude, and  $r$  is a random variable uniformly distributed between  $-1$  and  $1$ .

The calculations were conducted for different values of the ratio  $\lambda_0/W$ , the ratio  $\lambda/\lambda_0$ , and the reflection coefficient  $R$  at  $A = 2.5\lambda_0$  and  $A_n = 0.02$ . To get the maximum possible error, the initial phase  $\psi_0$  was chosen such that  $\Delta\phi_{er}(\psi_0) = \Delta\phi_{er \min}$ .

Fig. 3 shows the error  $\delta_{\max}$  versus ratio  $\lambda/\lambda_0$  for five cycles of vibration at  $W = 23$  mm,  $\lambda_0 = 3$  cm, and different values of the reflection coefficient  $R$ . As illustrated, at  $R > R_{0\min} = 1/\sqrt{2} \approx 0.71$  the error passes through a minimum, while at  $R < R_{0\min}$  it increases monotonically with  $\lambda/\lambda_0$ . Because of this, the error can be reduced by operating at  $\lambda_0$  if  $R < R_{0\min}$  and at a longer wavelength if  $R > R_{0\min}$ . As follows from Eq. (12), to the range of the actual reflection coefficient  $R$  from  $R_{0\min}$  to  $0.9$  (in free-space measurements, the reflection coefficient can hardly exceed  $0.9$ ) there corresponds the range of the measured reflection coefficient (the root  $R_2$ ) from  $2R_{0\min} - 0.9 \approx 0.514$  to  $0.9$ . So one should switch to an operating wavelength longer than  $\lambda_0$  only if the measured reflection coefficient exceeds  $0.514$ . An advisable value of the ratio  $\lambda/\lambda_0$  may be chosen such that the error  $\delta_{\max}$  averaged over the reflection coefficient range of  $0.514$  to  $0.9$  is a minimum. For  $W = 23$  mm and  $\lambda_0 = 3$  cm, the advisable ratio  $\lambda/\lambda_0$  is  $1.1$ .

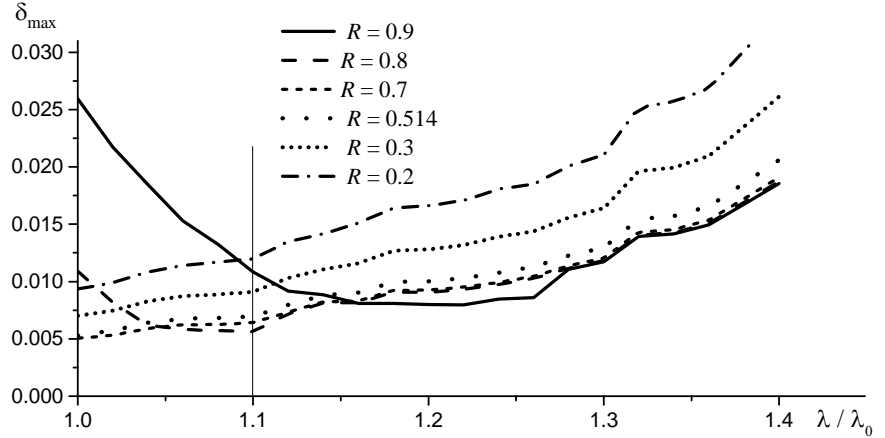


Fig. 3

In the existing technique [12], an interprobe distance of  $\lambda_g/10$  is used instead of the conventional  $\lambda_g/8$  in order to reduce the measurement error at reflection

coefficients close to unity. However, this may increase the measurement error if the reflection coefficient is rather small. Fig. 4 shows the difference  $\Delta$  of the maximum error  $\delta_{\max}$  for the conventional operating mode ( $l = \text{const} = \lambda_g/8$ ) and the maximum error  $\delta_{\max}$  for the proposed technique at  $W = 23$  mm,  $\lambda_0 = 3$  cm, and  $\lambda/\lambda_0 = 1.1$  and for the existing technique [12] ( $l = \text{const} = \lambda_g/10$ ). As illustrated, both techniques significantly reduce the error at reflection coefficients close to unity; however, the existing technique results in a marked increase in the error at rather small reflection coefficients, while the proposed technique is free from such a drawback.

Fig. 5 shows the advisable value of the ratio  $\lambda/\lambda_0$ ,  $(\lambda/\lambda_0)_{adv}$ , at which the error  $\delta_{\max}$  averaged over the reflection coefficient range of 0.514 to 0.9 is a minimum and the value of this minimum,  $(\bar{\delta}_{\max})_{\min}$ , versus the ratio  $\lambda_0/W$ . As can be seen from the figure, advisable values of the ratios  $\lambda/\lambda_0$  and  $\lambda_0/W$  may be chosen as  $\lambda/\lambda_0 = 1.1$  and  $1.3 \leq \lambda_0/W \leq 1.4$ .

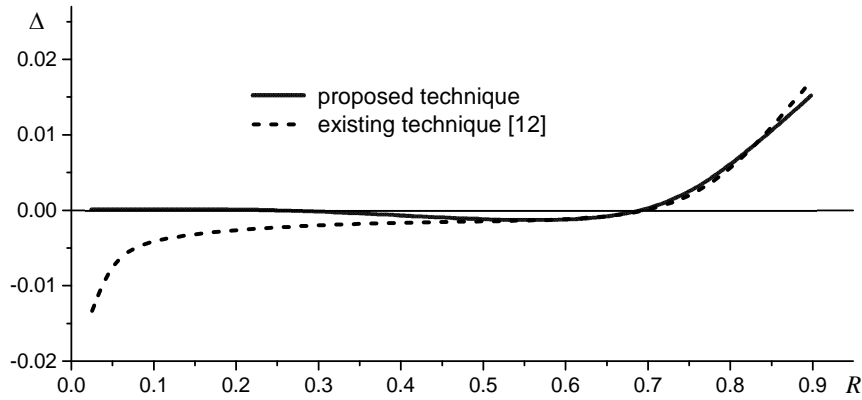


Fig. 4

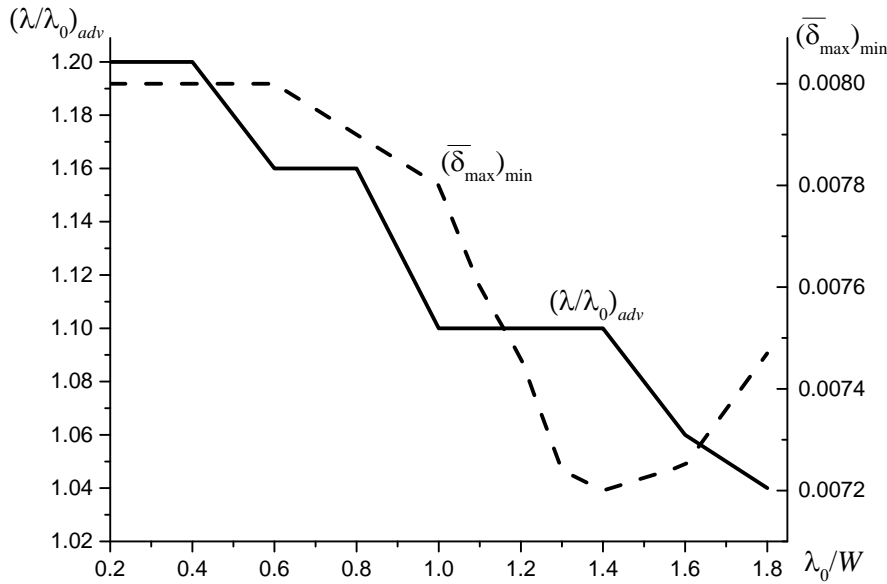


Fig. 5

Thus, in order to reduce the measurement error in a wide range of the reflection coefficient, the parameters  $\lambda_0$  (the free-space operating wavelength at which  $l = \lambda_g/8$ ) and  $W$  (the width of the waveguide section's broad wall) of a two-probe displacement meter should satisfy the condition  $1.3 \leq \lambda_0/W \leq 1.4$  m, and the free-space operating wavelength should switch from  $\lambda_0$  to  $1.1\lambda_0$  if the measured reflection coefficient exceeds 0.514.

The proposed method may be used in the development of microwave displacement sensors for various classes of vibration protection and workflow control systems.

1. Viktorov V. A., Lunkin B. V., Sovlukov A. S. Radiowave Measurements of Process Parameters. Moscow: Energoatomizdat, 1989. 208 pp. (in Russian).
2. Cunha A., Caetano E. Dynamic measurements on stay cables of stay-cable bridges using an interferometry laser system Experimental Techniques. 1999. V. 23. No. 3. Pp. 38–43. <https://doi.org/10.1111/j.1747-1567.1999.tb01570.x>
3. Kaito K., Abe M., Fujino Y. Development of a non-contact scanning vibration measurement system for real-scale structures. Structure and Infrastructure Engineering. 2005. V. 1, No 3. P. 189–205. <https://doi.org/10.1080/15732470500030661>
4. Mehrabi A. B. In-service evaluation of cable-stayed bridges, overview of available methods, and findings / A. B. Mehrabi // Journal of Bridge Engineering. 2006. V. 11, No 6. P. 716–724. [https://doi.org/10.1061/\(ASCE\)1084-0702\(2006\)11:6\(716\)](https://doi.org/10.1061/(ASCE)1084-0702(2006)11:6(716))
5. Lee J. J., Shinozuka M. A vision-based system for remote sensing of bridge displacement. NDT & E International. 2006. V. 39. No. 5. Pp. 425–431. <https://doi.org/10.1016/j.ndteint.2005.12.003>
6. Kim S., Nguyen C. A displacement measurement technique using millimeter-wave interferometry. IEEE Transactions on Microwave Theory and Techniques. 2003. V. 51. No. 6. Pp. 1724–1728. <https://doi.org/10.1109/TMTT.2003.812575>
7. Kim S., Nguyen C. On the development of a multifunction millimeter-wave sensor for displacement sensing and low-velocity measurement. IEEE Transactions on Microwave Theory and Techniques. 2004. V. 52. No. 11. Pp. 2503–2512. <https://doi.org/10.1109/TMTT.2004.837153>
8. Pylypenko O. V., Gorev N. B., Doronin A. V., Kodzhespirova I. F., Privalov E. N. Two-probe implementation of microwave interferometry for measuring the motion parameters of mechanical objects. Teh. Meh. 2013. No. 4. Pp. 112–122. (in Russian).
9. Tischer F. J. Mikrowellen-Messtechnik. Berlin: Springer-Verlag, 1958. 368 pp. <https://doi.org/10.1007/978-3-642-87504-5>
10. Cripps S. C. VNA tales. IEEE Microwave Magazine. 2007. V. 8. No. 5. Pp. 28–44. <https://doi.org/10.1109/MMM.2007.904719>
11. Andreev M. V., Drobakhin O. O., Saltykov D. Yu. Techniques of measuring reflectance in free space in the microwave range. Proceedings of the 2016 9<sup>th</sup> International Kharkiv Symposium on Physics and Engineering of Microwaves, Millimeter and Submillimeter Waves (MSMW), Kharkiv, Ukraine, June 20–24, 2016. Pp. 1–3. <https://doi.org/10.1109/MSMW.2016.7538213>
12. Pylypenko O. V., Gorev N. B., Doronin A. V., Kodzhespirova I. F. Motion sensing by a two-probe implementation of microwave interferometry. Teh. Meh. 2014. No. 4. Pp. 85–93. (in Russian).
13. Chavez S., Xiang Q.-S., An L., Understanding phase maps in MRI: A new outline phase unwrapping method. IEEE Transactions on Medical Imaging. 2002. V. 21. No. 8. Pp. 966–977. <https://doi.org/10.1109/TMI.2002.803106>
14. Hasar U. S., Barroso J. J., Sabah C., Kaya Y. Resolving phase ambiguity in the inverse problem of reflection-only measurement methods. Progress in Electromagnetics Research. 2012. V. 129. Pp. 405–420. <https://doi.org/10.2528/PIER12052311>
15. Silvia M. T., Robinson E. A. Deconvolution of Geophysical Time Series in the Exploration for Oil and Natural Gas. Amsterdam–Oxford–New York: Elsevier Scientific Publishing Company, 1979. 447 pp.

Received on 14.04.2020,  
in final form on 18.06.2020